Forest Chemicals Review
www.forestchemicalsreview.com
ISSN: 1520-0191
March-April 2022 Page No. 1095-1109
Article History: Received: 08 February 2022, Revised: 10 March 2022, Accepted: 02 April 2022, Publication: 30 April 2022

Numerical Analysis of Wind Load in Wind Environment of Construction Engineering by Computational Fluid Dynamics

Huijuan Hao*
Henan Technical College of Construction, Zhengzhou 450064, China
*Corresponding Author.

Abstract:

This study aims to reduce the threats to urban traffic and personal safety caused by wind environment problems such as "venturi effect" and "corner effect" formed between buildings in the process of urbanization. Firstly, based on Computational Fluid Dynamics (CFD), the wind environment model is built, meshed, parameterized, and solved. Then, the 270° wind direction is taken as an example to study the influence of wind environment on different building layouts. At present, three typical building groups in the city have been numerically simulated under different working conditions. Finally, the experiment obtained the results of the average wind speed, maximum wind speed, and safety range of different building layouts in the 270° wind direction. The results show that the wind load simulation can help people to study the different wind pressures formed in different areas of the building surface when different building layout structures face different inflow wind speeds, as well as the changes in the wind speed and safe area of the surrounding wind environment. Therefore, to fully understand the wind environment and wind load characteristics of different types of building complexes under strong wind conditions is of great significance for improving the planning and design level of building complexes, reducing the impact of strong winds on building complexes, and protecting pedestrian safety.

Keywords*: Computational Fluid Dynamics; building complex; wind environment; wind load; numerical simulation.*

I. INTRODUCTION

The wind is a natural phenomenon caused by airflow formed by the rotation of the earth on the surface of the earth. Human life is closely related to wind. The quality of human life also depends on the wind [1]. With the acceleration of China's urbanization process, in order to adapt to the rapidly growing population, buildings in cities continue to emerge, and the wind environment of buildings has become an important factor affecting the quality and safety of human life [2]. If the wind speed in the building complex is too small, it will cause problems such as poor ventilation and accumulation of pollutants; if the wind speed is too large, it will endanger the safety of pedestrians around the building and even cause damage to the building structure, causing huge losses to humans [3].

Forest Chemicals Review
www.forestchemicalsreview.com
ISSN: 1520-0191
March-April 2022 Page No. 1095-1109
Article History: Received: 08 February 2022, Revised: 10 March 2022, Accepted: 02 April 2022, Publication: 30 April 2022

However, although the rapidly emerging building groups effectively solve the problem of population living, there are also many wind environment problems, such as "narrow pipe effect" and "corner effect" [4, 5]. These environmental problems may not be of great concern to people when the wind speed is low, but when the wind speed increases, these problems usually directly threaten personal safety [6]. Therefore, the wind environment characteristics of different building complexes under high wind speed conditions are used to optimize the structure. Various building complexes can have a relatively safe wind environment in strong wind weather, reducing casualties and property losses [7].

Firstly, based on the Computational Fluid Dynamics (CFD) method, the wind environment model is built, meshed, parameterized, and solved. Then, the 270° wind direction is used as an example to carry out numerical simulations for different building layouts. Finally, the experiment obtained the average wind speed, maximum wind speed, and safety range of different building layouts in the 270° wind direction. These data provide technical support for fully understanding the wind environment and wind load characteristics of different types of building groups under strong wind conditions and are of great significance to improving the planning and design level of building groups, reducing the impact of strong winds on building groups, and protecting pedestrian safety. The innovation lies in the fact that it is based on the strong wind of level 8, which provides a certain reference for the planning and design of building complexes under strong wind conditions.

II. THEORY OF WIND FIELD OF BUILDING GROUP

2.1 Reasons for the formation of wind loads

The formation of wind load is caused by airflow, and the effect of wind load on buildings is irregular. Wind loads have random time-varying properties and are different from general live loads. Although wind noise can also affect buildings, the main effect is that wind loads affect the horizontal displacement of buildings [8].

2.2 Influence of wind load on high-rise buildings

The main load controlling super high-rise buildings is wind load. The three-dimensional wind load effect is generated by airflow over tall structures. It mainly includes vibration in three directions caused by transverse wind, longitudinal wind, and torsional wind loads [9]. The wind environment around high-rise buildings is determined by the flowing wind close to the ground, and the areas with poor wind environments are the corners of high-rise buildings and in roadways [10]. Although the longitudinal load has a large proportion in the building design, the horizontal load plays a decisive role [11]. For narrower high-rise buildings, wind loads can control the structural design. Its effect increases with the height of the building and often controls the load combination [12].

Forest Chemicals Review
www.forestchemicalsreview.com
ISSN: 1520-0191
March-April 2022 Page No. 1095-1109
Article History: Received: 08 February 2022, Revised: 10 March 2022, Accepted: 02 April 2022, Publication: 30 April 2022

2.3 CFD governing equations

The flow of any fluid in space must obey three basic laws of physics, namely, the law of conservation of mass, the law of conservation of momentum, and the law of conservation of energy. In CFD, it corresponds to the mass conservation equation, the momentum conservation equation, and the energy conservation equation [13,14].

2.3.1 Mass conservation equation

The physical meaning of the mass conservation equation is that the difference between the mass of the fluid flowing into the control body and the mass flowing out of the control body should be consistent with the increment of the fluid mass in the control body. According to Bernoulli's equation, when the air velocity is lower than 0.3 Mach number (about 102m/s), it can be considered incompressible. The mass conservation equation for an incompressible fluid and its density is constant is shown in Eq. (1):

$$\frac{\partial u}{\partial x}+\frac{\partial v}{\partial y}+\frac{\partial w}{\partial z}=0 \tag{1}$$

Among them, u, v, w are the components of velocity in x, y, z, in m/s.

2.3.2 Momentum conservation equation

The momentum conservation equation is also known as the Navier-Stokes equation or the N-S equation. The physical meaning is that in a given fluid system, the time rate of change of its momentum is equal to the synthesis of the external forces acting on it. The expression in the coordinate system is shown in Eqs. (2)-(4):

$$\rho\left(\frac{\partial u}{\partial t}+u\frac{\partial u}{\partial x}+v\frac{\partial u}{\partial y}+w\frac{\partial u}{\partial z}\right)=f_x-\frac{\partial P}{\partial x}+\mu\left(\frac{\partial^2 u}{\partial x^2}+\frac{\partial^2 u}{\partial y^2}+\frac{\partial^2 u}{\partial z^2}\right) \tag{2}$$

$$\rho\left(\frac{\partial u}{\partial t}+u\frac{\partial v}{\partial x}+v\frac{\partial v}{\partial y}+w\frac{\partial v}{\partial z}\right)=f_y-\frac{\partial P}{\partial y}+\mu\left(\frac{\partial^2 v}{\partial x^2}+\frac{\partial^2 v}{\partial y^2}+\frac{\partial^2 v}{\partial z^2}\right) \tag{3}$$

$$\rho\left(\frac{\partial w}{\partial t}+u\frac{\partial w}{\partial x}+v\frac{\partial w}{\partial y}+w\frac{\partial w}{\partial z}\right)=f_z-\frac{\partial P}{\partial z}+\mu\left(\frac{\partial^2 w}{\partial x^2}+\frac{\partial^2 w}{\partial y^2}+\frac{\partial^2 w}{\partial z^2}\right) \tag{4}$$

Among them, ρ is the fluid density, and the unit is kg/m^3. P is pressure. u, v, w are the velocity components of the fluid at point (x, y, z) at time t. f is the external force per unit volume of fluid. The constant μ is the dynamic viscosity.

2.3.3 Energy conservation equation

The physical meaning of the energy conservation equation is that the change of the total energy of a system can only be equal to the energy passed into or out of the system, as shown in Eq. (5):

Forest Chemicals Review
www.forestchemicalsreview.com
ISSN: 1520-0191
March-April 2022 Page No. 1095-1109
Article History: Received: 08 February 2022, Revised: 10 March 2022, Accepted: 02 April 2022, Publication: 30 April 2022

$$\frac{\partial}{\partial t}(\rho E)+\frac{\partial}{\partial x_i}[u_i(\rho E+p)]=\frac{\partial}{\partial x_i}\left[k_{eff}\frac{\partial T}{\partial x_i}-\sum_j' h_j' J_j'+u_j(\tau_{ij})_{eff}\right]+S_h \quad (5)$$

k_{eff} is the effective thermal conductivity, $k_{eff}=k+k_t$. k_t is the turbulent thermal conductivity. s_h is a term that includes the heat of chemical change reaction or other custom heat sources. E is the total energy in the microelement, the unit is J/kg, as shown in Eq. (6):

$$E=h-\frac{p}{\rho}+\frac{u^2}{2} \quad (6)$$

Where, h is the fluid baking value, h_j is the enthalpy value of the component j, defined as $h_j=\int_{T_{ref}}^{T} C_{p,j}dT$. Among them, T_{ref}=298.15K, the unit is J/kg.

2.4 Construction of the geometric model of the building complex

In studying wind environment and wind load of buildings, the construction of geometric model and mesh division is particularly important [15]. The geometric model needs to be as close as possible to the actual situation so that the real working conditions can be accurately simulated. The more commonly used building layout types in urban construction are selected for numerical simulation of wind fields. These three categories are determinant buildings, staggered buildings, and oblique buildings, as shown in Figure 1.

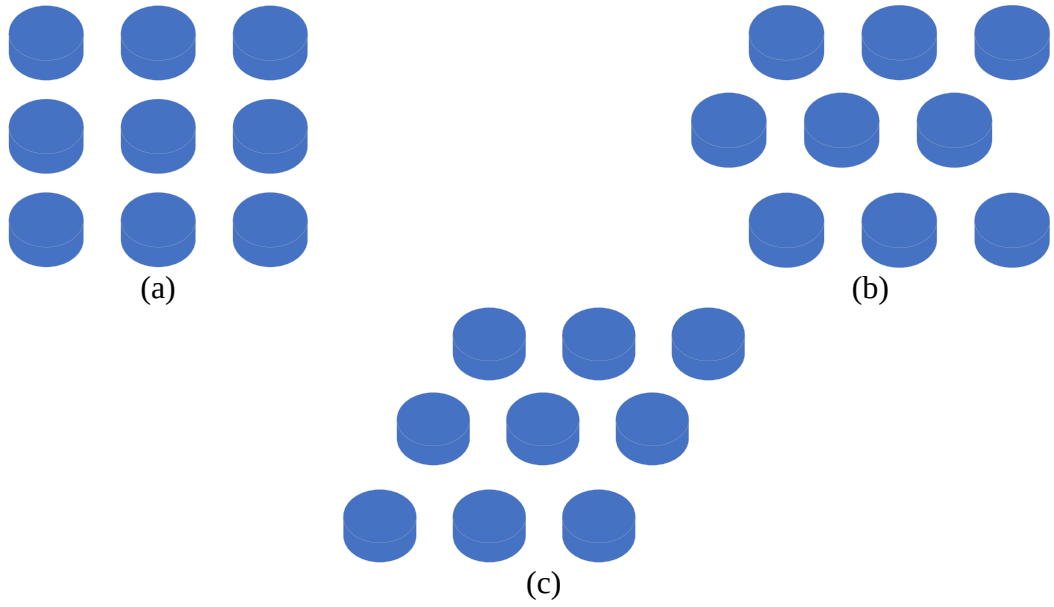

Figure 1: Layout of typical urban buildings ((a) determinant buildings (b) staggered buildings (c) oblique buildings)

The building layout determines the morphological characteristics of building groups, and the wind field

Forest Chemicals Review
www.forestchemicalsreview.com
ISSN: 1520-0191
March-April 2022 Page No. 1095-1109
Article History: Received: 08 February 2022, Revised: 10 March 2022, Accepted: 02 April 2022, Publication: 30 April 2022

characteristics of the layout of building groups with different morphological characteristics are also very different [16].

The International Federation of Chemical, Energy, Mine, and General Workers' Unions (ICEM CFD 15.0) software is selected for the geometric modeling of the complex. The diameter and height of the bottom surface of the single building are defined as 30m and 60m, respectively. This building model is used as a standard for combining base building complex models with different layout structures. The layout of determinant buildings is characterized by simple structure and strong regularity. Staggered building group: the second row of building models is moved at a distance of 30m vertically and 30m horizontally with reference to the position of the first row of building models. The third row of buildings is aligned with the first row of building models according to the longitudinal 90m spacing. Finally, three rows of buildings are staggered to form a standard staggered building complex geometric model with a 3×3 layout. Oblique building complex: after the first row of architectural models is assembled, the remaining two rows of architectural models are arranged in sequence at a distance of 30 m in the vertical direction and 30 m in the lateral direction, and finally, a standard slanted architectural complex geometric model with a 3×3 layout is formed [17-19].

2.5 Computational Domain Settings

The sizes of different computational domains are set according to different wind direction conditions. Wind directions of different conditions can be obtained by changing the position of the building group in the computational domain [20]. The different wind directions refer to the forward windward, oblique windward, and lateral windward of the building complex. The model layout of the building complex with symmetry is selected. Therefore, when the wind direction conditions are 270° wind direction (that is, the building group is facing the wind), 315° wind direction (that is, the building group is facing the wind obliquely) and 0° wind direction (that is, the building group is facing the wind sideways), three types of building groups can be covered all conditions in different wind directions.

The 270° wind direction is studied as an example, as shown in Figure 2.

Figure 2: Schematic diagram of the computational domain when the building complex is facing the wind

When the building complex is facing the wind (270° wind direction), the size of the computational

Forest Chemicals Review
www.forestchemicalsreview.com
ISSN: 1520-0191
March-April 2022 Page No. 1095-1109
Article History: Received: 08 February 2022, Revised: 10 March 2022, Accepted: 02 April 2022, Publication: 30 April 2022

domain is set to 1,800 m(X)×1,000 m(Y)×600 m(Z), respectively. The position of the windward side of the building group is set at 600m from the inflow surface of the computational domain, and the building group is set symmetrically along the central axis of the Y-axis.

The building complex is inclined to the wind (315° wind direction), as shown in Figure 3.

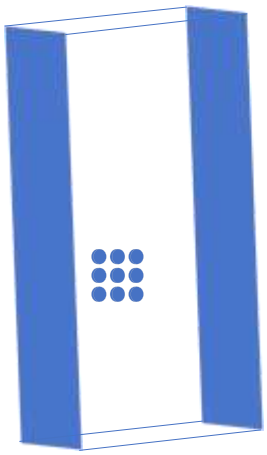

Figure 3: Schematic diagram of the computational domain when the building complex is inclined towards the wind

The computational domain is set to 1,800m(X) × 1,800m(Y) × 600m(Z). Because this type of computational domain contains two inflow surfaces, two windward surfaces of the building complex are set at a distance of 600m from the inflow surface of the computational domain.

The building complex faces the wind sideways (0° wind direction), as shown in Figure 4.

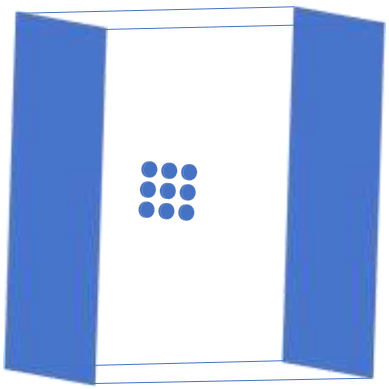

Figure 4: Schematic diagram of the computational domain when the building complex is facing the wind sideways

The computational domain size is set to 1,000m(X) × 1,800m(Y) × 600m(Z). The windward side of the

Forest Chemicals Review
www.forestchemicalsreview.com
ISSN: 1520-0191
March-April 2022 Page No. 1095-1109
Article History: Received: 08 February 2022, Revised: 10 March 2022, Accepted: 02 April 2022, Publication: 30 April 2022

building group is set at a distance of 600m from the inflow surface of the computational domain, and the building group is set symmetrically along the central axis of the X-axis.

The blocking rate of the computational domain can meet the requirements of the Japanese Architectural Society of Artificial Intelligence (AI) that the blocking rate of the computational domain is less than 3%. When the building complex is facing the wind in the forward direction and the lateral direction, the blocking rate of the computational domain is 1.5%. When the building complex is obliquely facing the wind, the blocking rate of the computational domain is about 0.83%.

2.6 Boundary condition setting

The boundary condition settings of the numerical simulation of the wind field of the building complex are consistent with those of the numerical simulation feasibility experiment. The boundary condition of the inflow surface of the computational domain is set to velocity-inlet. The boundary condition of the outflow surface of the computational domain is set to outflow. The building surface and ground shall adopt the non-slip wall. The top surface and other boundaries of the computational domain do not consider the influence of external flow, and there is no exchange of physical quantities such as mass and heat, so the symmetry is still used, as shown in Figure 5.

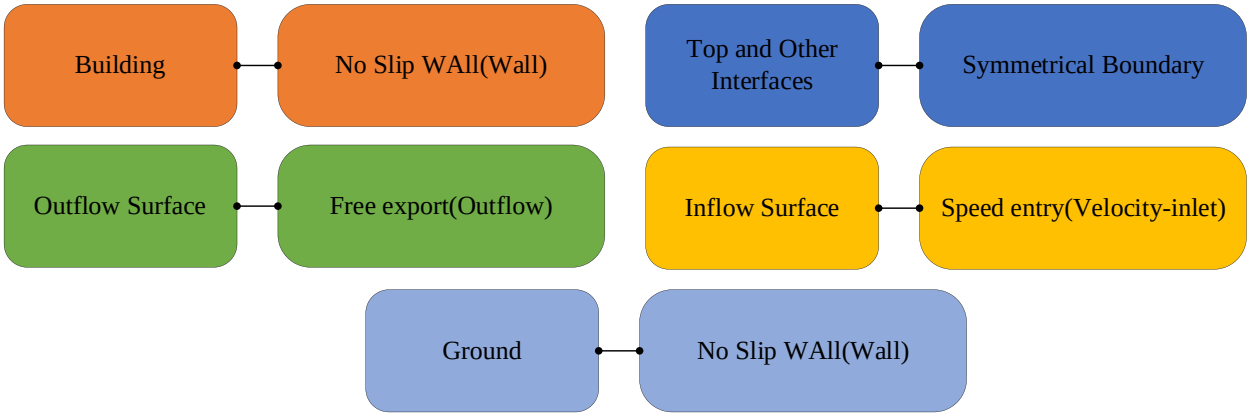

Figure 5: Boundary Condition Settings

The representative wind field environment in the urban modernization construction is the Class D wind field environment, so the numerical simulation of the wind field of the building group is still carried out in the Class D wind field environment. At the velocity inflow surface, the interface uses the UDF function and Fluent software design to define wind speed U, turbulent kinetic energy K, and dissipation rate ε.

III. EXPERIMENTAL RESULTS AND ANALYSIS

3.1 Verification of the horizontal homogeneity of the atmospheric boundary layer

Based on the RNK k-ε model, the wind speed at the height of 10 m on the inflow surface is set to 17.2m/s. The above scheme is selected to carry out numerical simulation in the empty computational

Forest Chemicals Review
www.forestchemicalsreview.com
ISSN: 1520-0191
March-April 2022 Page No. 1095-1109
Article History: Received: 08 February 2022, Revised: 10 March 2022, Accepted: 02 April 2022, Publication: 30 April 2022

domain under the condition of 270° wind direction, as shown in Figure 6.

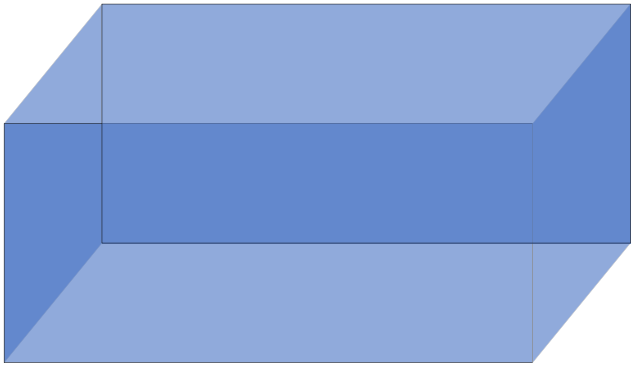

Figure 6: Empty computational domain under 270° wind direction

The computational domain is set to Y=500m. The calculation and analysis of the cross-section show that the distribution of the average wind speed in the computational domain is consistent with the exponential wind profile model, and the average wind speed in the horizontal direction does not change significantly.

3.2 Meshing and Independence Verification

This study verifies the determinant building complex with 270° wind and sets up three grid division schemes with different densities. The number of grids is 790,000, 1.23 million, and 2.01 million in sequence, and the flow field at the height of 1.5m for pedestrians is simulated in turn, as shown in Figure 7.

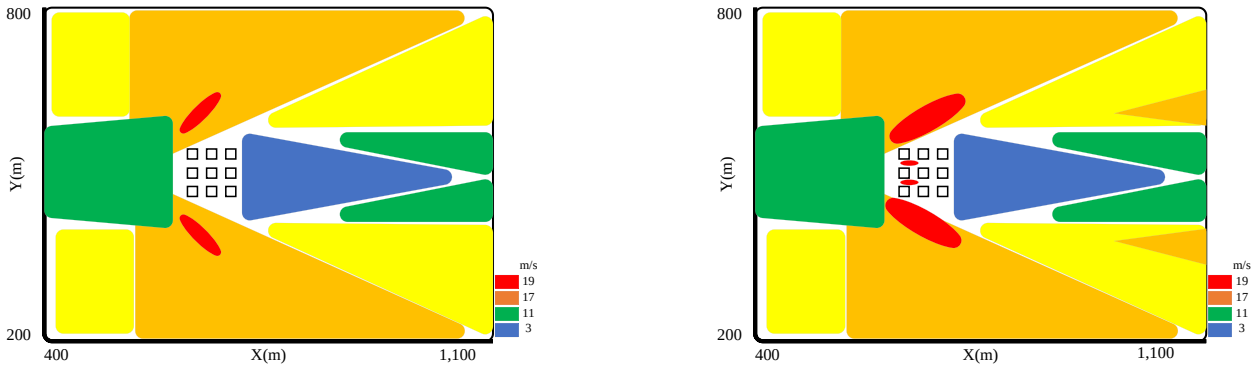

Forest Chemicals Review
www.forestchemicalsreview.com
ISSN: 1520-0191
March-April 2022 Page No. 1095-1109
Article History: Received: 08 February 2022, Revised: 10 March 2022, Accepted: 02 April 2022, Publication: 30 April 2022

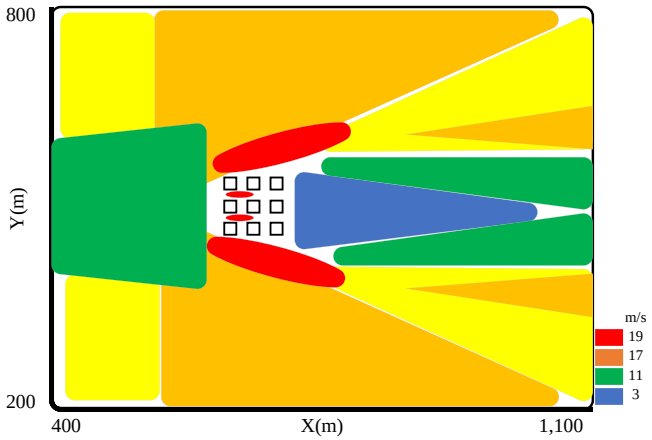

(c)

Figure 7: Schematic diagram of the wind speed cloud map obtained at a pedestrian height of 1.5m ((a) 790,000 grids (b) 1.23 million grids (c) 2.01 million grids)

In Figure 7, when the number of grids is 790,000 and 1.23 million, respectively, the simulation results of the two flow fields are significantly different, which are mainly reflected in the areas on both sides of the building complex and the wake area, as shown in Figure 7(a) and (b). When the number of grids is 2.01 million, there is no significant difference between it and 1.23 million.

3.3 Analysis of wind environment of buildings

When the wind direction is 270°, the wind speed cloud map at the pedestrian height (1.5m above the ground) of each building group is shown in Figure 8.

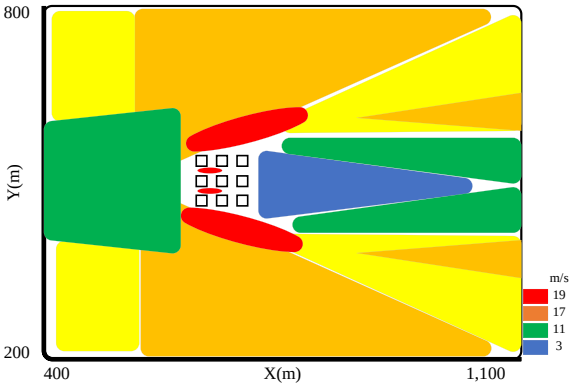

(a)

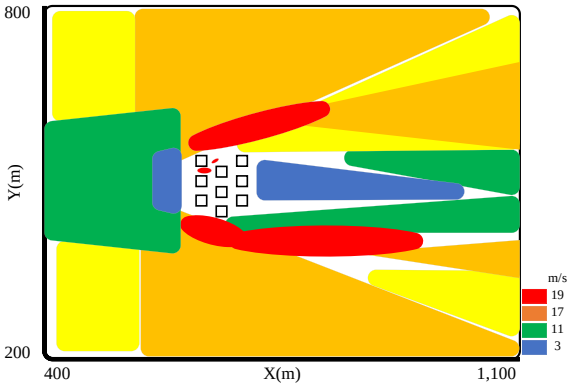

(b)

Forest Chemicals Review
www.forestchemicalsreview.com
ISSN: 1520-0191
March-April 2022 Page No. 1095-1109
Article History: Received: 08 February 2022, Revised: 10 March 2022, Accepted: 02 April 2022, Publication: 30 April 2022

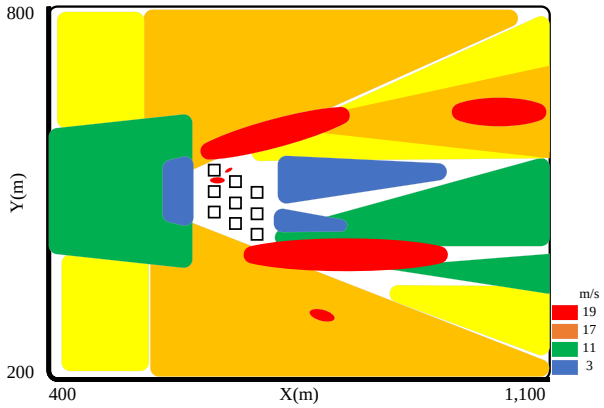

(c)

Figure 8: Distribution of wind speed at pedestrian heights for each building group in the 270° wind direction ((a) Matrix building group (b) Staggered building group (c) Oblique building group)

In Figure 8, when the air flows into a relatively narrow channel from an open place, the wind speed increases significantly, forming a "venturi effect". The determinant buildings are most seriously affected by the "venturi effect". The weakening of the wind speed at the channel is mainly because the wind will generate a vortex inside the determinant building complex and form a large wind shadow area. The staggered building group and the slanted building group are not affected by the "venturi effect", because the airflow in these two building groups has changed the original flow direction of the wind due to the staggered arrangement between the buildings.

When the wind faces the building complex from the front, all types of building complexes will form a wind shadow area on the leeward side of the building, that is, the area with lower wind speed. Among them, the wind speed in the wind shadow area of the determinant is lower, and the staggered building group and the slanted building group will affect the flow field due to the combination of buildings. Therefore, the wind speed in the formed wind shadow area is higher than that of the determinant building group, and only the wind shadow area with lower wind speed will be formed on the back of the building in the rear area of the building group.

When the airflow passes over the building complex from both sides, the airflow will separate at the outermost corner of the building complex. Therefore, the airflow will flow to both sides of the building complex, forming an area with high wind speed, often greater than 17m/s. Therefore, this area is called the hazardous wind speed area. This phenomenon is mainly affected by the building's complex structure and has little interaction with the buildings in the complex. The dangerous wind speed area of the determinant building complex is in the crosswind area, which is symmetrical along the X axis. Its length is equal to the length of the building complex. Although the dangerous wind speed areas of staggered buildings and inclined buildings are also on both sides, they have no symmetry, and the length is longer than that of determinant buildings and dissipates approximately within the wake area of the buildings.

Forest Chemicals Review
www.forestchemicalsreview.com
ISSN: 1520-0191
March-April 2022 Page No. 1095-1109
Article History: Received: 08 February 2022, Revised: 10 March 2022, Accepted: 02 April 2022, Publication: 30 April 2022

The wake area formed by the staggered building group and the inclined building group is affected by the interaction between the buildings, which is larger and more complex than that of the determinant building group and dissipates at about 1,100m of the X axis. The wake region of the determinant building complex dissipates at approximately 1,000m on the X axis.

The ratio of average wind speed, maximum wind speed, and safe area (wind speed less than 17m/s) in various building complexes and surrounding areas (referred to as building complex areas) with a wind direction of 270° is counted as shown in Figure 9.

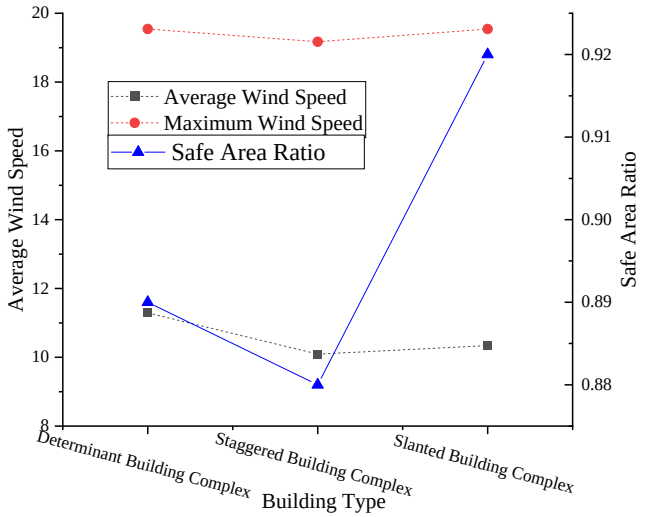

Figure 9: Simulation results of wind environment in each building area under 270° wind direction

In Figure 9, when the wind direction is 270°, the minimum average wind speed in the staggered building group is 10.09m/s. The maximum average wind speed in the determinant building group is 11.29m/s. The difference between the two is 1.2m/s. There is a maximum safe area with a proportion of 0.92 in the slanted building complex area. In addition, there is a minimum, maximum wind speed of 19.17m/s in the staggered building complex area. The maximum wind speed in the rest of the building complex is about 19.54m/s, with a small difference of about 0.37m/s.

Although the average wind speed and the maximum wind speed in the staggered building group are lower than those of the diagonal building group, the proportion of the safe area is slightly lower than that of the diagonal building group. This is mainly because the dangerous wind speed areas on both sides of the staggering buildings are larger than those of the inclined buildings, as shown in Figure 10.

Forest Chemicals Review
www.forestchemicalsreview.com
ISSN: 1520-0191
March-April 2022 Page No. 1095-1109
Article History: Received: 08 February 2022, Revised: 10 March 2022, Accepted: 02 April 2022, Publication: 30 April 2022

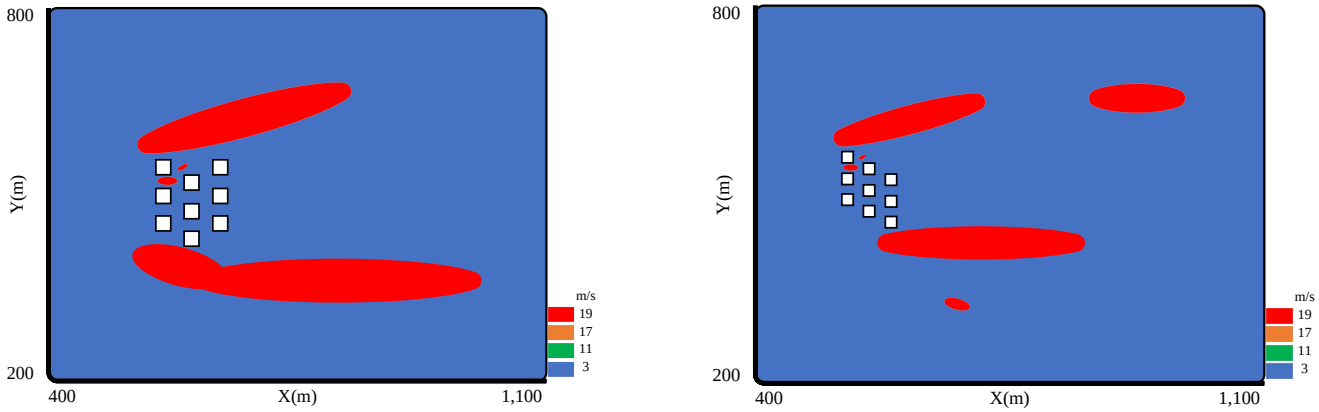

Figure 10: Distribution map of safe areas in the area of staggered buildings and slanted buildings with 270° wind down ((a) staggered buildings (b) slanted buildings)

Therefore, under the condition of 270° wind direction, when the average wind speed and maximum wind speed in the building group area cannot be ignored, the wind environment simulation results in the staggered building group area are the best. When the scale of the safe area in the building group area cannot be ignored, the wind environment simulation in the slanted building group area is the best.

3.4 Wind Load Analysis of Building Groups

Under the condition of 270° wind direction, the surface wind pressure distribution results of various buildings are shown in Figure 11.

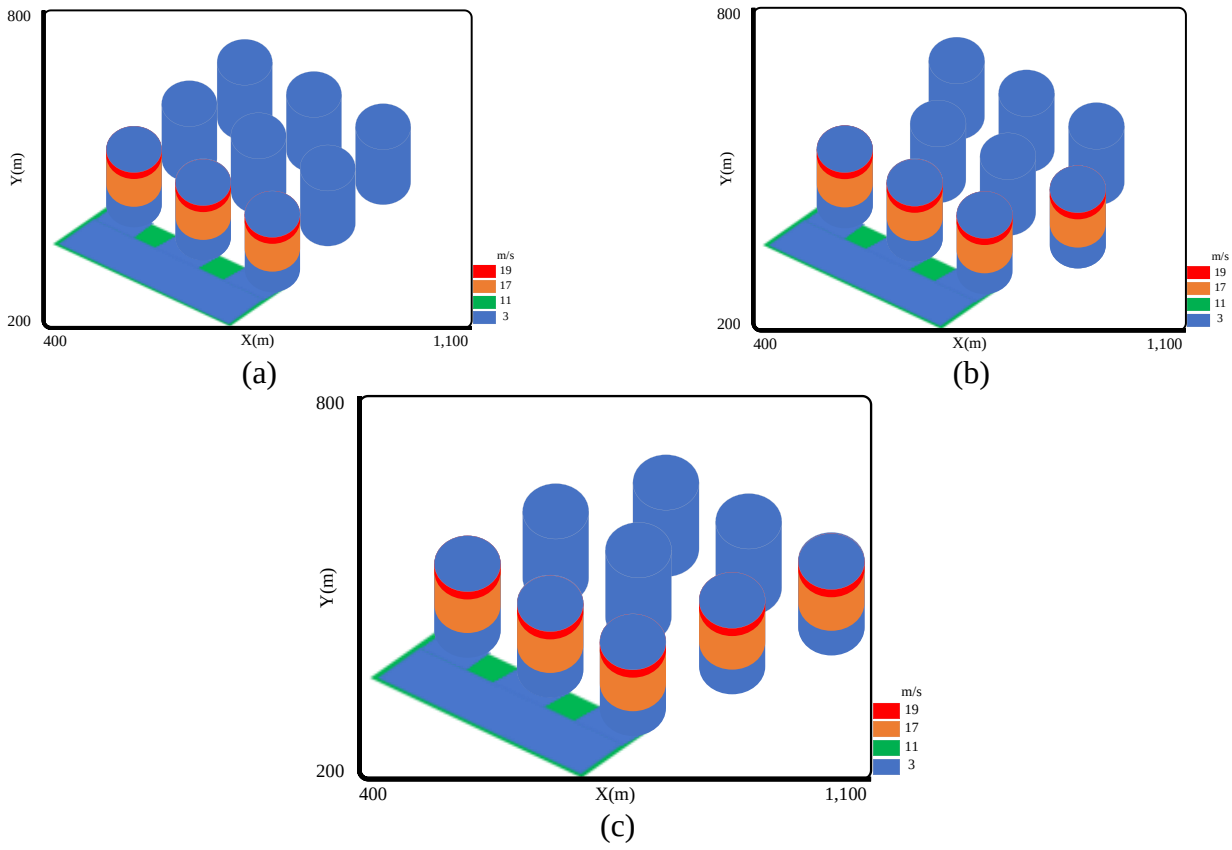

Figure 11: Distribution of surface wind pressure of each building group in 270° wind direction

Forest Chemicals Review
www.forestchemicalsreview.com
ISSN: 1520-0191
March-April 2022 Page No. 1095-1109
Article History: Received: 08 February 2022, Revised: 10 March 2022, Accepted: 02 April 2022, Publication: 30 April 2022

In Figure 11, when the wind faces each building group from the front, a positive pressure area will be formed on the surface of the windward building due to the extrusion of the airflow. When the airflow passes from the sides and the top of the building complex, the airflow at the corner of the building will generate vortices and generate greater suction. Therefore, the minimum wind pressure of all kinds of buildings appears in the top front edge area and the crosswind front edge area of the windward buildings. When the airflow reaches the leeward side of the building, a vortex will eventually be formed at the top area of the leeward side of the building, resulting in greater suction and a negative pressure area, as shown in Figure 12.

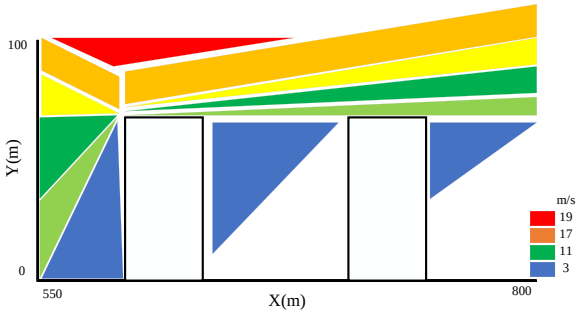

Figure 12: Schematic diagram of the flow field in the y=500m section of the determinant building complex

In Figure 12, the negative pressure on the downstream buildings in the building complex is relatively small, and the negative pressure on most of the facades is within the range of 0 to -100Pa. The negative pressure of the downstream buildings in the staggered building group and the slanted building group is higher than that of the determinant building group. The negative pressure in most areas of the building facades in the building complex is between -100Pa and -200Pa, and only a small part of the area is exposed to negative pressure in the range of 0-100Pa. Additionally, two types of staggered buildings and two types of oblique buildings also have a large negative pressure area within the wake area of the buildings. Its negative pressure is also in the range of -100Pa to -200Pa.

IV. CONCLUSION

In recent years, with the continuous advancement of the urbanization process, although many building clusters have effectively solved the problem of population living, they have also brought about wind environment problems such as "narrow pipe effect" and "corner effect". In windy weather, these problems directly threaten personal safety. In the D-type wind field environment, the representative model of the urban building group has been carried out in the numerical simulation study of the forward windward of the building group under the strong wind condition (17.2m/s). The wind environment is comprehensively evaluated from the three aspects of the average wind speed, the maximum wind speed and the area ratio of the safe area in the building group area. The results are analyzed and compared. Finally, the numerical simulation study of each building group under the forward wind is carried out to analyze the characteristics under different building group conditions and the relationship between the wind environment of each building group and the wind load simulation results. The innovation is that three typical building complexes in the current city are selected for numerical simulation research, with wide coverage and strong representativeness. However, there are still some deficiencies to be improved. The constructed

Forest Chemicals Review
www.forestchemicalsreview.com
ISSN: 1520-0191
March-April 2022 Page No. 1095-1109
Article History: Received: 08 February 2022, Revised: 10 March 2022, Accepted: 02 April 2022, Publication: 30 April 2022

models of various building groups are constructed of single buildings with the same height. The influence of buildings of different heights in the building group on the wind site of the building group is not considered. In the future, more building group combinations will be further studied. The selected inflow conditions are all ideal conditions without considering the impact caused by the surrounding buildings or complex terrain. Therefore, inflow conditions will be optimized for the specific case when conducting a real case analysis.

REFERENCES

[1] Boonstra, P. A., Wind, T. T., van Kruchten, M., Schuuring, E., Hospers, G. A., van der Wekken, A. J., ... & Reyners, A. K. (2020). Clinical utility of circulating tumor DNA as a response and follow-up marker in cancer therapy. *Cancer and Metastasis Reviews*, *39(3)*, 999-1013.

[2] Feng, W., Zhen, M., Ding, W., & Zou, Q. (2022). Field measurement and numerical simulation of the relationship between the vertical wind environment and building morphology in residential areas in Xi'an, China. *Environmental Science and Pollution Research*, *29(8)*, 11663-11674.

[3] Bokde, N., Feijóo, A., Villanueva, D., & Kulat, K. (2019). A review on hybrid empirical mode decomposition models for wind speed and wind power prediction. *Energies*, *12(2)*, 254.

[4] Jia, Y., Shang, L., Nan, J., Hu, G., Fang, Z. (2022). CFD Analysis of Fluid-Dynamic and Heat Transfer Effects Generated by a Fixed Electricity Transmission Line Interacting with an External Wind. *FDMP-Fluid Dynamics & Materials Processing, 18(2)*, 329–344.

[5] Feriduni, B., Farajzadeh, M. A., & Jouyban, A. (2019). Determination of Two Antiepileptic Drugs in Urine by Homogenous Liquid-Liquid Extraction Performed in A Narrow Tube Combined with Dispersive Liquid-liquid Microextraction Followed by Gas Chromatography-flame Ionization Detection. *Iranian Journal of Pharmaceutical Research: IJPR*, *18(2)*, 620.

[6] Li, Y., Li, Y. G., Li, Q. S., & Tee, K. F. (2019). Investigation of wind effect reduction on square high-rise buildings by corner modification. *Advances in Structural Engineering*, *22*(6), 1488-1500.

[7] Islam, M., Rahman, M., Chowdhury, M., Comert, G., Sood, E. D., & Apon, A. (2020). Vision-based personal safety messages (PSMs) generation for connected vehicles. *IEEE transactions on vehicular technology*, *69(9)*, 9402-9416.

[8] Coccia, M. (2021). The effects of atmospheric stability with low wind speed and of air pollution on the accelerated transmission dynamics of COVID-19. *International Journal of Environmental Studies*, *78(1)*, 1-27.

[9] Qin, G., Yan, Q., Zhu, J., Xu, C., & Kammen, D. M. (2021). Day-ahead wind power forecasting based on wind load data using hybrid optimization algorithm. *Sustainability*, *13(3)*, 1164.

[10] Lin, J., Xu, Y. L., Xia, Y., & Li, C. (2019). Structural Analysis of Large-Scale Vertical-Axis Wind Turbines, Part I: Wind Load Simulation. *Energies*, *12(13)*, 2573.

[11] Wang, Y., Ma, C. (2022). CFD-Based Numerical Analysis of the Thermal Characteristics of an Electric Vehicle Power Battery. *FDMP-Fluid Dynamics & Materials Processing, 18(1)*, 159–171.

[12] Wen, W., Gu, S., Xiao, B., Wang, C., Wang, J., Ma, L., ... & Guo, X. (2019). In situ evaluation of stalk lodging resistance for different maize (Zea mays L.) cultivars using a mobile wind machine. *Plant methods*, *15(1)*, 1-16.

Forest Chemicals Review
www.forestchemicalsreview.com
ISSN: 1520-0191
March-April 2022 Page No. 1095-1109
Article History: Received: 08 February 2022, Revised: 10 March 2022, Accepted: 02 April 2022, Publication: 30 April 2022

[13] Zhang, J. W., Wu, J. Q., Chen, W. R., Guan, J. F., Zhong, Y., & Xu, K. J. (2019). Simulation method for dropper dynamic load considering horizontal vibration behaviour. *International Journal of Simulation Modelling*, *8(4)*, 653.

[14] Mazzoni, L., Medori, I., Balducci, F., Marcellini, M., Acciarri, P., Mezzetti, B., & Capocasa, F. (2022). Branch Numbers and Crop Load Combination Effects on Production and Fruit Quality of Flat Peach Cultivars (Prunus persica (L.) Batsch) Trained as Catalonian Vase. *Plants*, *11(3)*, 308.

[15] Chandramouli, S., Farhat, A., & Musslimani, Z. H. (2022). Time-dependent Duhamel renormalization method with multiple conservation and dissipation laws. *Nonlinearity*, *35(3)*, 1286.

[16] Dehghani, M., & Samet, H. (2020). Momentum search algorithm: A new meta-heuristic optimization algorithm inspired by momentum conservation law. *SN Applied Sciences*, *2(10)*, 1-15.

[17] Jiang, C., Cai, W., & Wang, Y. (2019). A linearly implicit and local energy-preserving scheme for the sine-Gordon equation based on the invariant energy quadratization approach. *Journal of Scientific Computing*, *80(3)*, 1629-1655.

[18] Zhu, L., Wang, A., Jin, F. (2021). Using Image Processing Technology and General Fluid Mechanics Principles to Model Smoke Diffusion in Forest Fires. *FDMP-Fluid Dynamics & Materials Processing*, *17(6)*, 1213–1222.

[19] Light, A., & Miskelly, C. (2019). Platforms, scales and networks: meshing a local sustainable sharing economy. *Computer Supported Cooperative Work (CSCW)*, *28(3)*, 591-626.

[20] Muhammad, A. A., Yitmen, I., Alizadehsalehi, S., & Celik, T. (2019). Adoption of Virtual Reality (VR) for site layout optimization of construction projects. *Teknik Dergi*, *31(2)*, 9833-9850.